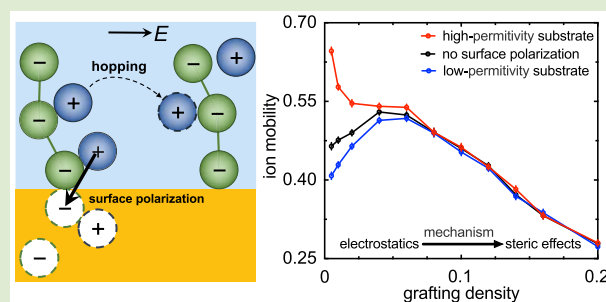


Dielectric Effects on Ion Transport in Polyelectrolyte Brushes

Jiaxing Yuan,^{†,‡,⊥} Hanne S. Antila,^{§,⊥} and Erik Luijten^{*,§,||,#,‡}[†]School of Physics and Astronomy and [‡]Institute of Natural Sciences, Shanghai Jiao Tong University, Shanghai 200240, China[§]Department of Materials Science and Engineering, ^{||}Department of Engineering Sciences and Applied Mathematics, and[#]Department of Physics and Astronomy, Northwestern University, Evanston, Illinois 60208, United States

Supporting Information

ABSTRACT: Surface-grafted polyelectrolytes provide a versatile way to create functionalized interfaces and nanochannels with externally controllable properties. Understanding the behavior of ions within the brush-like assemblies is crucial for the further development of these devices. We demonstrate that the ion transport through the brushes is governed by the interplay of electrostatic ion–polymer binding and steric effects, leading to a mobility that depends nonmonotonically on grafting density. However, the ion–polymer binding can be modulated by the dielectric properties of the substrate. As a result, surface polarization suppresses ion mobility near insulating interfaces and enhances it near conducting interfaces, even causing a shift from nonmonotonic to monotonic variation with grafting density.



Polyelectrolytes (PEs) can be end-grafted onto a substrate to form brush-like assemblies with a height and structure that respond to external stimuli, such as variation in temperature, pH, solvent quality, ionic strength, or chemical signals.^{1–3} The structural and functional variety of building blocks available makes the response highly customizable. Advances in manufacturing techniques have made it possible to graft polymers not only on outer surfaces, but also on the inner walls of nanopores, where the tunable charge density and the reversible collapse–extension transition of polyelectrolyte brushes (PEBs) can be employed to create nanoscale devices with controllable transport of solvent and solutes.^{4,5}

In particular, PEB-functionalized nanopores have the ability to regulate ionic flow by controlling the surface charge,⁵ which makes them potential building blocks for nanofluidic ionic circuits. This has been utilized to construct a synthetic analog⁶ to biological proton-gated channels, where conduction is switched on by PE protonation. In a similar fashion, nanochannels functionalized with a mixture of polyelectrolytes⁷ or zwitterionic brushes⁸ permit charge-selective conduction via inversion of surface charge or even ionic rectification.⁹ A voltage-gated rectifier has been demonstrated by grafting PEs¹⁰ to the opening of a nanochannel, where field reversal allows opening and closing the channel.

Despite the range of ion-transport characteristics exhibited by PEB-grafted nanopores, little is known about the mechanisms of ion conduction within the brushes. Hitherto, emphasis has primarily been on the transport of solvent^{11–14} and efforts to understand ion transport have not extended much beyond continuum treatments.¹⁵ Yet, microscopic information about the factors regulating ion conduction is crucial to further improve control over and efficiency of these

devices. A molecular theory¹⁶ has suggested that ion transport and molecular organization in the channels can be strongly coupled, especially for long polymers under high driving fields. This possible coupling makes particle-based simulations a powerful tool for investigating ion transport, as they enable a detailed view of both structure and dynamics of the system. Here, we take advantage of these capabilities and perform coarse-grained molecular dynamics (MD) simulations to (i) decipher the factors controlling the ion mobility in PEBs and (ii) demonstrate how ion mobility can be modulated by the dielectric properties of the substrate.

Our focus on substrate permittivity is motivated by the effect of surface polarization on the ion conductance of bare nanochannels containing a simple electrolyte. In recent simulations¹⁷ we uncovered a dielectric modulation of ion mobility that violates Kohlrausch's law. Remarkably, enhanced ion concentration near high-permittivity substrates is accompanied by increased ionic mobility, whereas the opposite occurs near low-permittivity surfaces. Furthermore, earlier calculations have predicted nanopore permittivity to alter number,^{18–20} distribution,²¹ and even type¹⁸ of ions within the channel through, for example, full dielectric exclusion²⁰ of ions or enhancement of ion selectivity.¹⁸ Yet, even though the materials used as PEB substrate range from insulating^{6,9} to conducting^{7,22} (even a thin metallic coating is sufficient to alter the substrate properties²³), the effect of substrate permittivity on PEBs remains an open question, apart from a study of PEB-grafted silica nanoparticles.²⁴

Received: November 13, 2018

Accepted: January 23, 2019

Our model system (Figure 1) consists of anionic PE oligomers, end-grafted in a square array to a planar substrate,

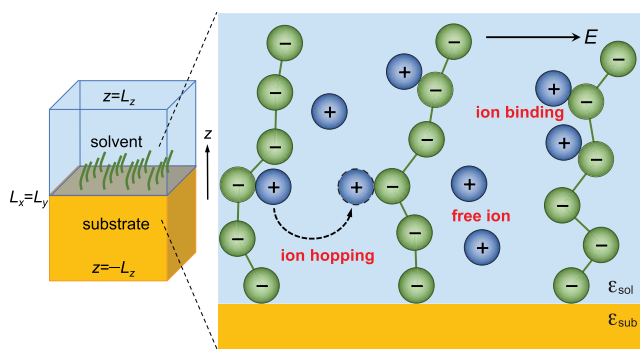


Figure 1. Schematic depiction of a polyelectrolyte brush. Polymers (green) are grafted onto a substrate with permittivity ϵ_{sub} and embedded in a solvent with permittivity ϵ_{sol} . Mobility of the counterions (blue) is probed via an external electric field E parallel to the substrate.

with monovalent ($q = e$) counterions. The polymers are modeled as bead–spring chains²⁵ of $N = 10$ monomers each carrying a charge $-q$. Ions and monomers are represented as spheres of diameter σ and mass m , interacting via a purely repulsive shifted-truncated Lennard-Jones (LJ) potential with coupling constant $\epsilon_{\text{LJ}} = k_{\text{B}}T/1.2$, where k_{B} is the Boltzmann's constant and T is the absolute temperature. The bonds between neighboring monomers are modeled as a harmonic potential $V_{\text{bond}} = (K/2)(r - r_0)^2$ with spring constant $K = 400\epsilon_{\text{LJ}}/\sigma^2$ and length $r_0 = 2^{1/6}\sigma$.

The ions and polymers are confined between purely repulsive LJ walls ($\epsilon_{\text{wall}} = \epsilon_{\text{LJ}}$; $\sigma_{\text{wall}} = 0.5\sigma$) at $z = 0$ and $z = L_z$ and immersed in an implicit solvent with dielectric permittivity ϵ_{sol} . The upper wall has permittivity equal to that of the solvent, whereas the PEB substrate at $z = 0$ has permittivity ϵ_{sub} . The permittivity difference at the solvent–substrate interface gives rise to surface polarization, which is dynamically taken into account in the MD simulations. Whereas complex geometries^{23,26} require a numerical solver,^{27,28} the planar interface makes it possible to treat polarization using the image-charge method,^{29,30} which we combine with the particle–particle particle–mesh Ewald summation.³¹ The magnitude and sign of the polarization is determined by the dielectric mismatch $\Delta = (\epsilon_{\text{sol}} - \epsilon_{\text{sub}})/(\epsilon_{\text{sol}} + \epsilon_{\text{sub}})$. A high-permittivity substrate carrying attractive polarization charges is characterized by $\Delta = -1$, $\Delta = +1$ represents a low-permittivity substrate with repulsive polarization charges, and $\Delta = 0$ reflects the absence of a dielectric mismatch.

As is customary for coarse-grained aqueous polyelectrolyte simulations,^{25,32} we adopt an enhanced Bjerrum length $l_{\text{B}} = e^2/(4\pi\epsilon_{\text{sol}}k_{\text{B}}T) = 3\sigma$. However, we will also examine how varying l_{B} affects ion conduction. We quantify the ion mobility $\mu = \langle v \rangle / (Eq)$ via the ensemble-averaged ion velocity $\langle v \rangle$ in the direction of the external electric field E that is applied parallel to the substrate and drives the ionic motion. The field strength employed, $E = 0.02\epsilon_{\text{LJ}}/(\sigma e)$, lies within the linear-response regime (Supporting Information, Figure S1). Further simulation details can be found in the Supporting Information (SI). Note that we opted to simulate short chains and moderate system sizes to allow extraction of high-quality data over various conditions with the available computational resources. However, we expect the general mechanisms observed to

remain valid for longer chains, and a comparison to larger systems was performed to ensure the absence of artifacts due to periodic boundary conditions. Our simulations do not include hydrodynamic interactions, molecular water, or additional salt, and we discuss the limitations of the model in connection to our results in the SI.

It is by no means a priori obvious how ion mobility will vary with PE grafting density Γ , even in the absence of surface polarization. In a simple electrolyte, bulk ion mobility decreases monotonically with increasing concentration. For a PEB, a larger concentration of (charged) monomers will modify the counterion concentration and distribution near the substrate, altering steric as well as electrostatic interactions. However, variation of the average separation between monomers of neighboring chains may also change the rate at which ions move through the channel. The potential complex interplay of these factors is confirmed in Figure 2a, which

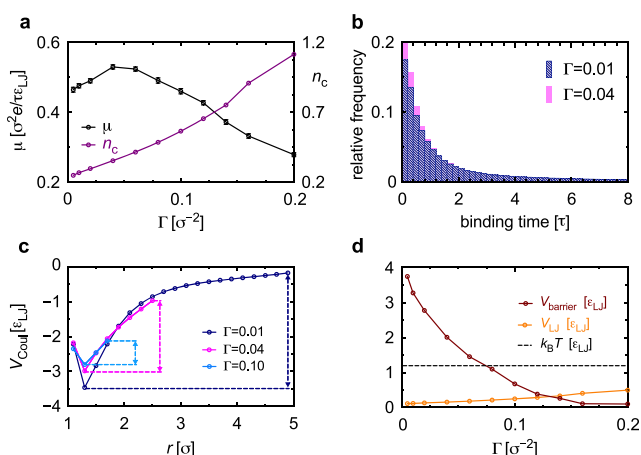


Figure 2. Mechanisms controlling ion mobility in a polyelectrolyte-coated nanochannel, in the absence of dielectric mismatch. (a) Average ion mobility μ and number of ion–particle contacts n_c . Remarkably, μ depends nonmonotonically on grafting density Γ . (b) Relative frequency distribution of binding times for $\Gamma = 0.01\sigma^{-2}$ and $\Gamma = 0.04\sigma^{-2}$ suggests enhanced ion mobility when grafting density is increased in the regime of low Γ . Binding time is defined as the time interval between ion attachment ($r \leq 2\sigma$) to a polymer chain and successive detachment. (c) Ensemble-averaged ionic electrostatic energy V_{Coul} as a function of distance r to the chain demonstrates the energy barrier for ion hopping between chains. The variation of this barrier with Γ explains the increase in hopping frequency in (b). (d) Average excluded-volume energy of ion–particle contacts V_{LJ} and the electrostatic energy barrier V_{barrier} as a function of Γ . The dashed horizontal line marks $k_{\text{B}}T = 1.2\epsilon_{\text{LJ}}$.

reveals that ion mobility depends nonmonotonically on grafting density, initially increasing with Γ before turning over to a decreasing trend. To explain this nonmonotonicity, we examine how varying grafting density alters the dynamics of ion–polymer binding under a driving field in the regime of low Γ . There, an increase in Γ lowers the ion–polymer binding time (Figure 2b), signaling that bound ions more readily detach from the chains and contribute to free conduction.

The decrease in binding time can be understood from the underlying energy landscape. To unbind, ions must overcome the electrostatic barrier $V_{\text{barrier}} \equiv \langle V_{\text{Coul}}(r_{\text{max}}) - V_{\text{Coul}}(r_{\text{min}}) \rangle$, where $\langle V_{\text{Coul}}(r) \rangle$ is the ensemble-averaged total electrostatic energy of an ion at separation r from its nearest monomer. The

separation r_{\min} corresponds to the energy minimum, whereas the largest separation of an ion located between two neighboring chains is accurately approximated by its 2D projection, $r_{\max} \approx (2\sqrt{\Gamma})^{-1}$. Fluctuations in brush conformation evidently have the potential to lower V_{barrier} , but Figure 2c shows that V_{Coul} indeed increases monotonically up to r_{\max} , resulting in a barrier height that decreases with increasing grafting density. This is analogous to the enhancement of ion mobility with increasing monomer density observed in polyelectrolyte hydrogels.³³ The dependence of V_{barrier} on grafting density (Figure 2d) also explains the reversal in mobility around $\Gamma = 0.05\sigma^{-2}$. Maximum mobility occurs when the decreasing V_{barrier} becomes comparable to the thermal energy $k_{\text{B}}T$. Beyond this threshold, mobility is dominated by steric interactions (cf. the rise in particle–particle contacts, Figure 2a, and the concomitant increase in excluded-volume energy V_{LJ} , Figure 2d) and, hence, decreases with increasing Γ .

To our knowledge, this nonmonotonic dependency of ion mobility on PE grafting density and the underlying mechanism have not been reported before. However, the motivation for the present work goes beyond this, as we aim to elucidate to what extent dielectric mismatch between the solvent and the substrate affects these observations. Induced surface polarization charge proves to have drastic consequences for the μ – Γ relationship. Figure 3a illustrates that, in the regime of low

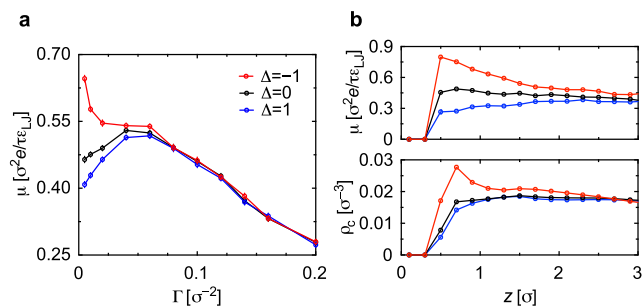


Figure 3. Ion mobility is affected by the dielectric properties of the polyelectrolyte-grafted substrate. (a) Average ion mobility as a function of brush grafting density Γ for different values of dielectric mismatch Δ . $\Delta = -1$ represents a high-permittivity (metallic) surface and $\Delta = +1$ represents a low-permittivity substrate. (b) Ion mobility (top) and density (bottom) profiles as a function of distance z to the substrate for $\Gamma = 0.01\sigma^{-2}$. The mobility and distribution profiles are truncated at $z = 3\sigma$ to focus on the dielectric effects occurring at the interface. Data for the full z -range are presented in Supporting Information, Figure S3.

grafting density, low-permittivity substrates suppress ion mobility, whereas high-permittivity substrates significantly enhance it. At higher Γ , we do not observe this dielectric modulation. As a result, a low-permittivity substrate further amplifies the nonmonotonicity of ion mobility with Γ , but when the PEB is grafted on a metallic surface the maximum in $\mu(\Gamma)$ can even disappear altogether.

At low grafting density, variation in ϵ_{sub} can result in nearly a 2-fold increase in ion mobility, far higher than the differences reported for bare nanochannels.¹⁷ To elucidate the origin of this observation, we examine the ion mobility (Figure 3b, top) and ion density (Figure 3b, bottom) profiles as a function of distance to the substrate.

As both properties are modulated in the same interfacial region, it is tempting to seek a causal relationship. However,

such an explanation encounters various obstacles. Straightforward application of Kohlrausch's law for ion mobility would predict a decrease in mobility with increasing concentration,^{34–36} the opposite of our observations. In fact, already the nonmonotonicity of the global mobility in the nonpolarizable case (Figure 2a) calls the applicability of this law into question. In addition, Figure 3b shows that low-permittivity substrates suppress ion mobility without significantly affecting the ion density profile. The observations in this figure qualitatively persist at higher grafting densities (Supporting Information, Figure S2). Their decrease in magnitude owing to electrostatic screening, along with the dominance of steric effects, explains why mobility is unaffected by substrate permittivity for higher grafting densities, $\Gamma > 0.075$. Note that variation in steric effects, caused by polarization-induced changes in interfacial ion and monomer concentrations, does not play a significant role in the dielectric modulation of ion mobility, as further discussed in the SI.

What, then, is the origin of the observed ion mobilities near PEB-functionalized polarizable substrates? Whereas the mobilities in Figure 3b and Supporting Information, Figure S2 behave in a manner remarkably similar to those of a simple electrolyte in a nanochannel,¹⁷ in such systems the mobility is regulated by the shape and size of the counterion cloud around each ion, a situation manifestly different from ion transport in a PEB, which relies on a single mobile species as charge carrier. Instead, we employ the framework established in Figure 2 to clarify the observed phenomenon. As illustrated in Figure 4a–c, the spatial distribution of counterions in the interfacial region is strongly affected by dielectric contrast. At $\Delta = 0$ (no polarization effects, Figure 4b), the ions are clustered around the grafted polyelectrolytes. This nonuniformity of the ion

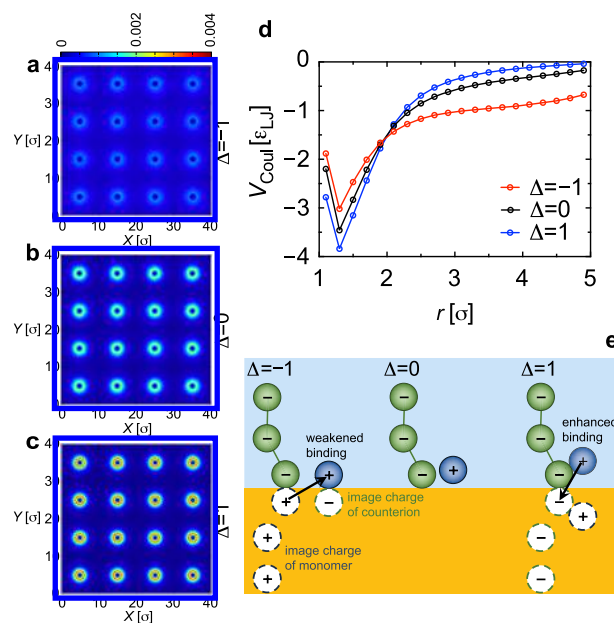


Figure 4. Effect of surface polarization on ion–polymer interactions. Normalized ion distribution near the interface ($z \leq 1.5\sigma$) for $\Gamma = 0.01\sigma^{-2}$ and (a) $\Delta = -1$, (b) $\Delta = 0$, and (c) $\Delta = 1$. (d) Average electrostatic energy around the polymer near the interface for $\Gamma = 0.01\sigma^{-2}$. (e) Ion–polymer binding is modulated by a dielectric three-body effect, where ions interact with the polarization charge (presented here as image charge) induced by the polymer they are bound to.

distribution is enhanced in the presence of a low-permittivity substrate ($\Delta = +1$, Figure 4c). Conversely, a high-permittivity substrate ($\Delta = -1$) suppresses this clustering, yielding a far more even distribution (Figure 4a). The electrostatic energy barrier, encountered by ions that hop from chain to chain, decreases as the mismatch is varied from $\Delta = +1$ to $\Delta = -1$ (Figure 4d), matching the observed variation in ion–polymer binding and consistent with the enhancement in ion transport.

The origin of the modulation of ion–polymer binding by surface polarization is explained most concisely in terms of image charges. Figure 4e illustrates a three-body effect on an ion bound to a monomer, whereby the ion interacts with the polarization charge induced by the monomer it is bound to. Near a conducting substrate ($\Delta = -1$), this secondary interaction is repulsive and weakens the ion–polymer binding. In contrast, monomer-induced polarization of a low-permittivity substrate ($\Delta = +1$) enhances the ion–polymer binding. Interestingly, this mechanism bears resemblance to the modulation of ion transport in confined, simple electrolytes,¹⁷ where surface polarization deforms the counterion cloud surrounding each ion. We also note connections to the predicted dependence of ion–ion interactions on surface polarization,³⁷ supported by the experimental observation of enhanced ion dissociation and conduction of a weak electrolyte near a high-permittivity interface.³⁸

The magnitude of the ion mobility as well as its sensitivity to dielectric mismatch depend on the electrostatic interaction. The strength of this interaction, often quantified via the Manning parameter $\xi = l_B \lambda$,³⁹ where $-e\lambda$ denotes the polymer charge per unit length, will affect the conformation of the brush, the number of ions in the brush, and their interaction with the monomers and the polarization charges. In the results above, we set $l_B = 3\sigma$ and $\lambda = (2^{1/6}\sigma)^{-1}$, that is, $\xi \approx 2.67$. This strong interaction means that the fraction of ions residing in the brush, while slightly affected by Γ , always exceeds 93%.

We proceed to adjust ξ in two distinct ways, namely by changing l_B (variation of either solvent permittivity or temperature, Supporting Information, Figure S4a) and by scaling the monomer charges (varying λ , Supporting Information, Figure S4b), and explore the resulting ion mobilities and fluxes along with the underlying PEB structure and ion distribution. Even though the brush conformation and ion distribution depend on the manner in which ξ is tuned, the resulting ion mobilities are very similar (Supporting Information, Figure S4a,b, middle panels), decreasing monotonically in both scenarios. However, the ion flux differs greatly, with an increase in Bjerrum length reducing the flux proportionally to the mobility, but an increase in polymer charge implying a growth in the number of counterions that overwhelms the reduction in mobility (Figure S4a,b, bottom panels).

Regardless of how ξ is varied, the strongest dielectric effects are observed at large ξ . At large Bjerrum length, this arises because the monomers and ions experience a stronger electrostatic interaction with the polarization charges. For high polymer charge, it occurs because the magnitude of the polarization charges increases accordingly. The modulation of ion mobility observed in Figure 3 is qualitatively similar for the entire range of Manning parameter examined. Quantitatively, the effect of metallic substrates is stronger than of low-permittivity substrates.

In summary, we have demonstrated that the ion mobility within polyelectrolyte brushes, a system with significant

applications in ion flow control on the nanoscale, is governed by electrostatic ion–polymer binding in sparse brushes and by steric effects in dense brushes, leading to a nonmonotonic dependence on grafting density. However, these observations change in the presence of dielectric mismatch between the solvent and the substrate, as ion mobility is modified by the emergence of surface polarization at the fluid–substrate interface. Using molecular simulations we have elucidated how this dielectric modulation occurs via a three-body effect, where ions in the interfacial region interact with the surface polarization charge induced by the polyelectrolytes they are bound to. As a result, ion transport is accelerated near a high-permittivity substrate and decelerated near a low permittivity substrate. This effect is more pronounced at lower grafting densities, so that the nonmonotonic relationship between mobility and grafting density is enhanced in polyelectrolyte brushes grafted on a low-permittivity substrate and suppressed in a brush on a conducting interface. By providing insight into fundamental mechanisms of ion transport, these results can contribute to the design of functional devices that allow precise control over ion transport on the nanoscale.

■ ASSOCIATED CONTENT

📄 Supporting Information

The Supporting Information is available free of charge on the ACS Publications website at DOI: 10.1021/acsmacrolett.8b00881.

Simulation details, additional characterization, and model limitations (PDF).

■ AUTHOR INFORMATION

Corresponding Author

*E-mail: luijten@northwestern.edu.

ORCID

Jiaying Yuan: 0000-0001-9890-4961

Hanne S. Antila: 0000-0002-2474-5053

Erik Luijten: 0000-0003-2364-1866

Author Contributions

[†]These authors contributed equally.

Notes

The authors declare no competing financial interest.

■ ACKNOWLEDGMENTS

This material is based upon work supported by the U.S. National Science Foundation under Grant No. DMR-1610796.

■ REFERENCES

- (1) Cohen Stuart, M. A.; Huck, W. T. S.; Genzer, J.; Müller, M.; Ober, C.; Stamm, M.; Sukhorukov, G. B.; Szleifer, I.; Tsukruk, V. V.; Urban, M.; Winnik, F.; Zauscher, S.; Luzinov, I.; Minko, S. Emerging applications of stimuli-responsive polymer materials. *Nat. Mater.* **2010**, *9*, 101–113.
- (2) Azzaroni, O. Polymer brushes here, there, and everywhere: Recent advances in their practical applications and emerging opportunities in multiple research fields. *J. Polym. Sci., Part A: Polym. Chem.* **2012**, *50*, 3225–3258.
- (3) Tagliazucchi, M.; Szleifer, I. Stimuli-responsive polymers grafted to nanopores and other nano-curved surfaces: structure, chemical equilibrium and transport. *Soft Matter* **2012**, *8*, 7292–7305.
- (4) Adiga, S. P.; Brenner, D. W. Stimuli-responsive polymer brushes for flow control through nanopores. *J. Funct. Biomater.* **2012**, *3*, 239–256.

- (5) Tagliazucchi, M.; Szeleifer, I. Transport mechanisms in nanopores and nanochannels: can we mimic nature? *Mater. Today* **2015**, *18*, 131–142.
- (6) Yameen, B.; Ali, M.; Neumann, R.; Ensinger, W.; Knoll, W.; Azzaroni, O. Synthetic proton-gated ion channels via single solid-state nanochannels modified with responsive polymer brushes. *Nano Lett.* **2009**, *9*, 2788–2793.
- (7) Motornov, M.; Tam, T. K.; Pita, M.; Tokarev, I.; Katz, E.; Minko, S. Switchable selectivity for gating ion transport with mixed polyelectrolyte brushes: Approaching ‘smart’ drug delivery systems. *Nanotechnology* **2009**, *20*, 434006.
- (8) Silies, L.; Andrieu-Brunsen, A. Programming ionic pore accessibility in zwitterionic polymer modified nanopores. *Langmuir* **2018**, *34*, 807–816.
- (9) Yameen, B.; Ali, M.; Neumann, R.; Ensinger, W.; Knoll, W.; Azzaroni, O. Single conical nanopores displaying pH-tunable rectifying characteristics. Manipulating ionic transport with zwitterionic polymer brushes. *J. Am. Chem. Soc.* **2009**, *131*, 2070–2071.
- (10) Harrell, C. C.; Kohli, P.; Siwy, Z.; Martin, C. R. DNA–nanotube artificial ion channels. *J. Am. Chem. Soc.* **2004**, *126*, 15646–15647.
- (11) Harden, J. L.; Long, D.; Ajdari, A. Influence of end-grafted polyelectrolytes on electro-osmosis along charged surfaces. *Langmuir* **2001**, *17*, 705–715.
- (12) Hickey, O. A.; Holm, C.; Harden, J. L.; Slater, G. W. Influence of charged polymer coatings on electro-osmotic flow: Molecular dynamics simulations. *Macromolecules* **2011**, *44*, 9455–9463.
- (13) Chen, G.; Das, S. Electroosmotic transport in polyelectrolyte-grafted nanochannels with pH-dependent charge density. *J. Appl. Phys.* **2015**, *117*, 185304.
- (14) Gao, X.; Zhao, T.; Li, Z. Controlling flow direction in nanochannels by electric field strength. *Phys. Rev. E* **2015**, *92*, 023017.
- (15) Zeng, Z.; Yeh, L.-H.; Zhang, M.; Qian, S. Ion transport and selectivity in biomimetic nanopores with pH-tunable zwitterionic polyelectrolyte brushes. *Nanoscale* **2015**, *7*, 17020–17029.
- (16) Tagliazucchi, M.; Rabin, Y.; Szeleifer, I. Ion transport and molecular organization are coupled in polyelectrolyte-modified nanopores. *J. Am. Chem. Soc.* **2011**, *133*, 17753–17763.
- (17) Antila, H. S.; Luijten, E. Dielectric modulation of ion transport near interfaces. *Phys. Rev. Lett.* **2018**, *120*, 135501.
- (18) Boda, D.; Valiskó, M.; Eisenberg, B.; Nonner, W.; Henderson, D.; Gillespie, D. The effect of protein dielectric coefficient on the selectivity of a calcium channel. *J. Chem. Phys.* **2006**, *125*, 034901.
- (19) Balme, S.; Picaud, F.; Manghi, M.; Palmeri, J.; Bechelany, M.; Cabello-Aguilar, S.; Abou-Chaaya, A.; Miele, P.; Balanzat, E.; Janot, J. M. Ionic transport through sub-10 nm diameter hydrophobic high-aspect ratio nanopores: experiment, theory and simulation. *Sci. Rep.* **2015**, *5*, 10135.
- (20) Buyukdagli, S.; Manghi, M.; Palmeri, J. Ionic exclusion phase transition in neutral and weakly charged cylindrical nanopores. *J. Chem. Phys.* **2011**, *134*, 074706.
- (21) Zhang, B.; Ai, Y.; Liu, J.; Joo, S. W.; Qian, S. Polarization effect of a dielectric membrane on the ionic current rectification in a conical nanopore. *J. Phys. Chem. C* **2011**, *115*, 24951–24959.
- (22) Guo, W.; Xia, H.; Xia, F.; Hou, X.; Cao, L.; Wang, L.; Xue, J.; Zhang, G.; Song, Y.; Zhu, D.; Wang, Y.; Jiang, L. Current rectification in temperature-responsive single nanopores. *ChemPhysChem* **2010**, *11*, 859–864.
- (23) Wu, H.; Han, M.; Luijten, E. Dielectric effects on the ion distribution near a Janus colloid. *Soft Matter* **2016**, *12*, 9575–9584.
- (24) Tergolina, V. B.; dos Santos, A. P. Effect of dielectric discontinuity on a spherical polyelectrolyte brush. *J. Chem. Phys.* **2017**, *147*, 114103.
- (25) Hsiao, P.-Y.; Luijten, E. Salt-induced collapse and reexpansion of highly charged flexible polyelectrolytes. *Phys. Rev. Lett.* **2006**, *97*, 148301.
- (26) Wu, H.; Li, H.; Solis, F. J.; Olvera de la Cruz, M.; Luijten, E. Asymmetric electrolytes near structured dielectric interfaces. *J. Chem. Phys.* **2018**, *149*, 164701.
- (27) Barros, K.; Sinkovits, D.; Luijten, E. Efficient and accurate simulation of dynamic dielectric objects. *J. Chem. Phys.* **2014**, *140*, 064903.
- (28) Wu, H.; Luijten, E. Accurate and efficient numerical simulation of dielectrically anisotropic particles. *J. Chem. Phys.* **2018**, *149*, 134105.
- (29) Thomson, W. Geometrical investigations with reference to the distribution of electricity on spherical conductors. *Camb. Dublin Math. J.* **1848**, *3*, 141–148.
- (30) Jackson, J. D. *Classical Electrodynamics*, 3rd ed.; Wiley: New York, 1999.
- (31) Hockney, R. W.; Eastwood, J. W. *Computer Simulation Using Particles*; IOP Publishing: Bristol, 1988.
- (32) Stevens, M. J.; Kremer, K. The nature of flexible linear polyelectrolytes in salt free solution: A molecular dynamics study. *J. Chem. Phys.* **1995**, *103*, 1669–1690.
- (33) Li, H.; Erbaş, A.; Zwanikken, J.; Olvera de la Cruz, M. Ionic conductivity in polyelectrolyte hydrogels. *Macromolecules* **2016**, *49*, 9239–9246.
- (34) Kohlrausch, F. Das elektrische Leitungsvermögen der wässrigen Lösungen von den Hydraten und Salzen der leichten Metalle, sowie von Kupfervitriol, Zinkvitriol und Silbersalpeter. *Ann. Phys. (Berlin, Ger.)* **1878**, *242*, 1–210.
- (35) Debye, P.; Hückel, E. Zur Theorie der Elektrolyte. II. Das Grenzgesetz für die elektrische Leitfähigkeit. *Phys. Z.* **1923**, *24*, 305–325.
- (36) Onsager, L. Zur Theorie der Electrolyte. II. *Phys. Z.* **1927**, *28*, 277–298.
- (37) Nadler, B.; Hollerbach, U.; Eisenberg, R. S. Dielectric boundary force and its crucial role in gramicidin. *Phys. Rev. E: Stat. Phys., Plasmas, Fluids, Relat. Interdiscip. Top.* **2003**, *68*, 021905.
- (38) Korobeynikov, S. M.; Melekhov, A. V.; Solovitchik, Y. G.; Royak, M. E.; Agoris, D. P.; Pyrgioti, E. Surface conductivity at the interface between ceramics and transformer oil. *J. Phys. D: Appl. Phys.* **2005**, *38*, 915–921.
- (39) Manning, G. S. Limiting laws and counterion condensation in polyelectrolyte solutions I. Colligative properties. *J. Chem. Phys.* **1969**, *51*, 924–933.